Journal of Peptide Science, Vol. 3, 415–428 (1997)

Solution Structure Determination of Endothelin-1 in Methanol/Water by NMR and Molecular Modelling Methods

CHANDRALAL M. HEWAGE, LU JIANG, JOHN A. PARKINSON, ROBERT RAMAGE and IAN H. SADLER

Department of Chemistry, University of Edinburgh, Edinburgh EH9 3JJ, UK

Received 14 December 1996
Accepted 10 February 1997

Abstract: To understand the structural requirements for the biological activity of endothelin peptides and to develop receptor selective endothelin analogues further, the solution structure of the bicyclic 21 amino acid residue vasoactive peptide, endothelin-1, has been determined in methanol-d_3/water using high-resolution ^{1}H-NMR spectroscopy. To our knowledge, this solvent system has not previously been used in NMR studies of endothelin and/or endothelin-like peptides. Two-dimensional DQFCOSY, TOCSY and NOESY spectra were acquired along with a series of one-dimensional spectra. A total of 219 distance constraints and 5 angle constraints were derived from the NMR data. These were incorporated into structure calculations using distance geometry (DIANA) followed by simulated annealing and molecular dynamics. The resulting structures are characterized by an α-helical conformation, Lys^9-His^{16}, and residues Ser^5-Asp^8 form a type I β-turn. The N-terminal region, which was not extensively constrained by NMR data, showed no preferred conformation. The C-terminal tail showed less extensive conformational averaging but no descriptive conformation could be observed. The results obtained in this study are in good agreement with previous proposals. ©1997 European Peptide Society and John Wiley & Sons, Ltd.

J. Pep. Sci. 3: 415–428,
No. of Figures: 7. No. of Tables: 3. No. of Refs: 58

Keywords: Endothelin-1; molecular modelling; solution structure

INTRODUCTION

Endothelin-1 (ET-1, **1**; Figure 1) was originally discovered in the supernatant liquid of cultured bovine aortic endothelial cells and was subsequently isolated from the supernatant liquid of a porcine aortic endothelial cell culture [1]. This potent vasoconstrictor peptide released from endothelial cells has attracted great interest as one possible candidate for endothelium-derived vasoconstrictor factors (EDCF) [2]. Owing to its long-lasting vasopresser effects [3], ET-1 has been proposed to mediate vasoconstriction via the production of EDCF in response to various chemical and physical stimuli. ET-1 belongs to a peptide class of mammalian origin in which the sequence of this peptide has been highly conserved during the course of vertebrate evolution and may perform similar homeostatic functions in a variety of mammalian and non-mammalian species. The primary sequence of human endothelin (**1**) was deduced from a human placental cDNA library and found to be identical to that of porcine endothelin, now referred to as

Abbreviations: DIANA, distance geometry algorithm for NMR applications; DQFCOSY, double quantum filtered correlation spectroscopy; DSA, dynamical simulated annealing; ET-1, endothelin-1; MD, molecular dynamics; RMSD, root mean square deviation; TOCSY, total correlation spectroscopy.

Address for correspondence: Ian H. Sadler, Department of Chemistry, University of Edinburgh, King's Buildings, West Mains Road, Edinburgh EH9 3JJ, UK

CCC 1075-2617/97/060415-14

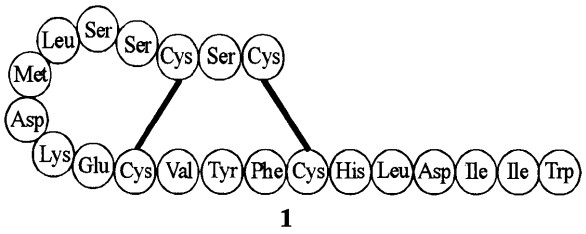

1

Figure 1 The primary structure of ET-1.

endothelin-1 [4]. Over the past seven years this peptide has drawn the attention of many investigators because of its unique structure and important biological actions.

Numerous studies have been reported on the pharmacological evaluation of endothelin analogues and fragments [5, 6]. Structure–activity relationship studies of endothelin and its analogues have been reviewed extensively [7, 8]. After careful consideration of the literature reports published on biological and pharmacological evaluation of endothelins, we decided to investigate this area further. In order to understand the basic structural requirements for biological activity, the solution structure of endothelin-1 was investigated. Characteristic properties of ET-1 are the conserved disulphide bridges, Cys^{1}-Cys^{15} and Cys^{3}-Cys^{11}, and the hydrophobic amino acid residues at the tail region which are believed to be important for its biological activities. It is well known that the truncated and linear ET-1 analogues produce unpromising biological activity [9] which suggests that the overall structure of ET-1 is essential for its activity.

Most peptides are normally found in aqueous environments and water would therefore be a natural choice of solvent in which to study the peptide structure. However, peptides act at protein surfaces or in membranes that are a less polar environment and therefore a less polar solvent should give a more meaningful result in these cases. Less polar solvents also tend to induce more structure in peptides because of the weaker capacity of the solvent to engage in hydrogen bonding with the peptide [10]. Either methanol or trifluoroethanol (TFE) is often added to aqueous solutions to induce helix formation, the assumption being that the helices seen in such solvent systems are representative of the helices formed in their native environment, particularly in membranes.

In our studies, therefore, a 1:1 mixture of methanol-d_3 and water has been used as the solvent. This mixture is frequently used in HPLC analysis, and it offers two advantages. Firstly the peptide displays good solubility properties in the mixture and secondly the solvent contains half the amount of protonated water which eases to some extent the dynamic range problem normally associated with NMR experiments undertaken in water as solvent. ET-1 has a rather low molecular weight and in solution it showed monodispersity without any detectable aggregation under the experimental conditions used for the NMR experiments.

ET-1 was synthesized in our laboratory and folded using a novel protocol. It was found to have potent biological activity consistent with previously reported results [11]. Here a complete sequence-specific assignment of ^{1}H-NMR data from ET-1 and its three-dimensional structure derived from NOESY data using molecular modelling techniques is presented. It is shown that the results are in good agreement with previous reports on solution conformational studies of ET-1 in different solvents and solvent mixtures. Further investigations of a series of modified endothelin-1 analogues are being investigated.

MATERIALS AND METHODS

Peptide Synthesis

The peptide was synthesized on the adapted ABI 430A Peptide Synthesizer using Fmoc chemistry of a 0.25 mmol scale and Wang resin was used as the solid supporter. The amino acid side-chain protections were: OtBu (Asp, Glu), tBu (Ser, Tyr), Boc (Lys), Trt (His, Cys). The Fmoc group was deprotected with 20% piperidine in dimethylformamide (DMF). Acetylation was carried out in a solution of 0.5 M acetic anhydride, 0.125 M diisopropylethylamine (DIEA) and 0.2% HOBt in DMF. The deprotection of Fmoc was monitored by an on-line ultraviolet monitoring system.

All residues were incorporated by double couple cycles using the 1-hydroxyl-4-ethoxycarbonyl-1,2,3-triazole (HOCt) active ester method. The only exception was histidine which was coupled through its 1-hydroxybenzotriazole ester (HOBt) due to increased racemization with HOCt. In each cycle, one cartridge containing 0.5 mmol Fmoc amino acid was used and the active ester was formed via the addition of 0.5 mmol diisopropylcarbodiimide. The completed peptide was cleaved from the resin with a mixture of TFA:EDT:thioanisole:TIS:H_2O (10:1:0.5:0.2:0.5). The crude peptide was precipitated from ether after removing the TFA *in vacuo*.

The crude, fully reduced peptide (80 mg) was dissolved in 6 M guanidine.HCl (200 ml), which contained 0.1 M Tris buffer (pH 8, 20 °C), GSSG (0.5 mM) and GSH (5 mM). The mixture was stirred at room temperature overnight and purified twice using a C18 preparative column, eluting with a linear gradient of 0.1% TFA/H_2O with increasing concentration of 0.1% TFA/CH_3CN at 5 ml/min. The correct fraction was concentrated and dried by lyophilization to give 15.5 mg ET-1 (yield 19.4% from crude peptide).

This peptide was characterized under different analytical HPLC conditions (RP C18, Vydac C18 and Hichrom C18 columns). MS m/z 2489.3 ($C_{109}H_{159}N_{25}O_{32}S_5$, requires 2490.0). A co-injection with commercial human ET-1 (Peptide Institute Inc., Japan) showed a single sharp peak.

NMR Spectroscopy

All NMR experiments were performed using a 5 mm proton (inverse) probe on a Varian VXR 600S spectrometer operating a proton resonance frequency of 599.945 MHz. Samples were examined in 5 mm Wilmad 528PP NMR tubes. The residual ^{1}H-NMR signal from CD_2HOH was used as an internal reference and defined as 3.30 ppm. The spectrometer was controlled with a Sun4/110 host computer using the VNMR system software version 4.1. The white solid peptide sample (5 mg), ET-1, was dissolved in 1:1 CD_3OH:H_2O (700 μl) except for amide proton exchange studies. One-dimensional ^{1}H-NMR data and the two-dimensional ^{1}H-DQFCOSY, TOCSY and NOESY data sets were acquired. A similar peptide sample dissolved in 1:1 = CD_3OD:D_2O was used for amide proton exchange studies. All the NMR experiments were performed on the sample at pH 3.6 and 298 K except for variable temperature studies.

One-dimensional NMR data were recorded with a presaturation delay of 1 s. Some 256 transients were acquired over a 7 kHz spectral width into 35000 data points. The data were zero filled to 65,536 data points and were apodized using an optimized shifted squared sinebell function prior to Fourier transformation.

Two-dimensional phase-sensitive DQFCOSY [12], TOCSY [13] and NOESY [14] data sets were acquired with a presaturation delay of 1.5 s and an eight-step phase cycle scheme. The MLEV-17 'clean-TOCSY' spin-lock pulse sequence was used with an 80 ms mixing time cycle and two trim pulses of 2 ms each. A series of NOESY data sets with different mixing times (40, 80, 150, 200, 300 ms) were collected and evaluated for the effects of spin-diffusion and the NOESY data of ET-1 acquired with 150 ms mixing time were used for the structure determination. The water signal was saturated during the preparation and mixing periods. Some 32, 16 and 32 transients were acquired for each of 2×256 t_1 increments (hypercomplex acquisition) [15] into 2048 complex data points for the DQFCOSY, TOCSY and NOESY data respectively. Other acquisition parameters for all three data sets were: acquisition time 0.146 s; spectral width 7 KHz. Fourier transformation in F_2 was carried out without zero filling whereas data were zero filled to 1024 data points in F_1 prior to Fourier transformation. All the data sets were apodized in both dimensions using an optimized shifted squared sinebell window function. The real Fourier transformation was carried out on 1024×2048 data points. All the 2D spectra were acquired on a non-spinning sample.

Variable temperature studies of the peptide sample were carried out on a solution of 1 mg of the peptide using a standard one-dimensional ^{1}H-NMR pulse sequence. Spectra were recorded progressively at 4°; intervals from 290 to 298 K and 5 °; from 298 to 318 K. Amide proton-deuterium exchange experiments were carried out soon after dissolving the peptide sample using 1 mg of the peptide and standard one-dimensional ^{1}H-NMR spectra were acquired. A relaxation delay of 1.5 s was used only during the preparation period to eliminate the residual HOD solvent resonance. Data were recorded at 5 min intervals (15–20 min), 10 min intervals (20–50 min), 15 min intervals (50–80 min), 30 min intervals (80-140 min), 1 hr intervals (140–260 min) and 2 hr intervals (260–740 min) consecutively 2 min after the submission of the sample into the magnet.

Molecular Modelling

Structure calculation studies were carried out using the Tripos molecular modelling software [16] and SYBYL version 6.1 was used. The NOESY data of ET-1 acquired with 150 ms mixing time were processed using the same recipes as those used for manipulating data for structure determinations. The NOESY cross peaks that were not extensively overlapped were selected manually. Volume integrals and NOESY connectivity assignment columns were then used for generating lower and upper distance constraints. Dipolar couplings were classified into three categories of upper distance bounds according

to their volume integral values 2.8 Å (strong), 3.6 Å (medium) and 5.0 Å (weak). The lower distance bound was in all cases set to the van der Waals distance of 1.8 Å. The threshold values of upper distance bounds were established using the known sequential distances of d_{NN} and $d_{\alpha N}$ [17]. Pseudo-atoms with appropriate distance corrections were employed for protons that could not be stereospecifically assigned [18]. In the case of partial signal overlap, tentative assignments were ignored in the structure calculation.

The disulphide bridges of ET-1, Cys^{1}–Cys^{15} and Cys^{3}-Cys^{11} were fixed directly in all structure calculations by constraining a distance of 2.0–2.1 Å on the S_i–S_j bond and 3.0–3.1 Å on the $^{\beta}C$-$S_{i/j}$ bond across each bridge [19]. Slow amide proton exchange rates observed for some NHs in the helical region of the peptide backbone were used to constrain these NH protons and the relevant backbone carbonyl inter-atomic distances by introducing hydrogen bonds in the ranges of 1.8–2.0 Å and 2.7–3.0 Å for the H–O distance and N–O distance respectively [19]. Torsion angle (ϕ) constraints were generated from the $3J_{HN\alpha}$ coupling constants of the amide protons (< 5.5 Hz).

An initial structure was built using SYBYL and the distance geometry program DIANA [20] was used to generate random starting structures. The 211 distance constraints obtained from the NOESY cross-peak volumes were used as input for the DIANA calculation. Six constraints across the disulphide bridges, eight constraints for hydrogen bonds and five torsional angle constraints were also incorporated. All distance and torsional constraints were included in DIANA calculations. During the DIANA calculation, atomic distances were constrained using the force constant $k_{NOE} = 1$ kcal/mol/Å^2 and torsions were constrained using $k_{Dihed\_c} = 0.01$ kcal/mol/deg^2. DIANA was used to calculate 300 structures from random starting conformations and the calculation produced 25 best structures dependent on the final target function value. Distances that are predetermined by the covalent geometry of the molecule or by conformations that will violate the constraints are regarded as irrelevant in the DIANA program. These constraints were eliminated during the calculation and 131 structurally important constraints were produced as modified bounds.

The output structures from the DIANA calculation were then constrained by these modified distance bounds. In these structures, inter-atomic distances were constrained using a higher force constant of $k_{NOE} = 10$ kcal/mol/Å^2 and torsions were constrained using the same force constant $k_{Dihed\_c} = 0.01$ kcal/mol/deg^2. Structures were then subjected to 200 steps of conjugate-gradient energy minimization.

The conjugate-gradient optimization method was the method of choice for energy minimization in all structure calculations. Higher energies were minimized using an atom-by-atom Simplex minimization. The Tripos 5.2 force field with the standard Sybyl energy minimizer MAXIMIN 2 were used in the minimization program. Other parameters for constraining covalent geometry were $k_{Bond} = 600$ kcal/mol/Å^2, $k_{Angle} = 0.02$ kcal/mol/deg^2, and $k_{Tor} = 0.2$ kcal/mol/deg^2. Further details of the parameters are discussed by Clark *et al.* [21].

Energy-minimised structures were then refined using the dynamical simulated annealing (DSA) method adopted by Tripos molecular modelling software, DSA being a process by which local energy minima are overcome by successive heating and cooling cycles of the molecular model. The DSA process was started at the maximum temperature of 1000 K and the system was held at that temperature for 5400 fs. During the annealing time of 900 fs, the temperature was reduced until the minimum temperature of 100 K was reached. The Boltzmann scaling of atomic velocities were chosen from a random number seed and the 'stepwide' annealing method was used during the cooling period. This process completed the first cycle, and ten cycles were run altogether for each structure. The conformations obtained by DSA were further minimized with 200 steps of conjugate-gradient energy minimization. The minimization parameters used were the same as those described for the DIANA calculated structures.

The energy-minimized conformations were subjected to a final molecular dynamics (MD) quenching calculation without changing either distance or torsional force constants. The MD calculations were performed in the gas phase. The initial atomic velocities were chosen from a random distribution at 1000 K and the dynamic trajectory (100 fs) was followed for 20 ps in 1 fs steps. These calculations were carried out under NTV ensemble conditions with a 10 fs coupling factor for the temperature. The molecular dynamics calculations were repeated three times for each conformation using different initial values for random number seed (2×10^4, 6×10^4, 1×10^5) to obtain three different conformers for each starting conformations. These three different conformers were then averaged to obtain

the averaged conformation. After removing all the distance and torsional experimental energy barriers, these averaged conformers were finally subjected to 500 steps of conjugate-gradient energy minimization as described previously.

RESULTS AND DISCUSSION

The major problem involved in the synthesis of endothelin peptides is the correct formation of the two disulphide bonds. Random oxidation of the fully reduced peptides normally affords a mixture of two different isomers, (1–15, 3–11) and (1–11, 3–15), in a ratio of 3:1 [22, 23]. Methods have been developed for regioselective disulphide formation [24] and orthogonal cysteine protection [25] has also been introduced. However, the yields for such procedures were either very poor or not reported.

A new method was developed for the synthesis of ET-1. The peptide chain of ET-1 was assembled by double coupling cycles using a newly developed coupling reagent HOCt [26]. All four cysteins were protected with triphenylmethyl group. The coupling percentage was greatly improved and the crude peptide afforded was of very high purity according to the HPLC analysis. The folded ET-1 was purified by HPLC and characterized by amino acid analysis, MS, analytical HPLC and a co-injection of the purified peptide with commercial ET-1. The biological activity of the synthetic ET-1 was also comparable with the native ET-1.

The importance of the biologically active structure of a peptide in determining the specific receptor interactions and eliciting its pharmacological properties has made the three-dimensional structure of the endothelins a subject of intense interest. ET-1 displays well-defined, high-resolution, proton NMR spectra in aqueous CD_3OH. Furthermore, a significant spread in the chemical shifts has also been observed. Despite the low molecular mass of ET-1, a large number of NOEs were recorded, all of which were negative.

The sequence of 21 residues in ET-1 includes eight unique amino acids, Met^7, Lys^9, Glu^{10}, Val^{12}, Tyr^{13}, Phe^{14}, His^{16} and Trp^{21}. The two disulphide bridges that make the bicyclic core at the N-terminus region are formed at positions 1–15 and 3–11. The finger print region of the DQFCOSY spectrum (F_2,F_1) showed 20 cross peaks for all the NH/αH connectivities except the N-terminus residue, Cys^1. This cross peak was absent owing to the rapid exchange of the amide proton.

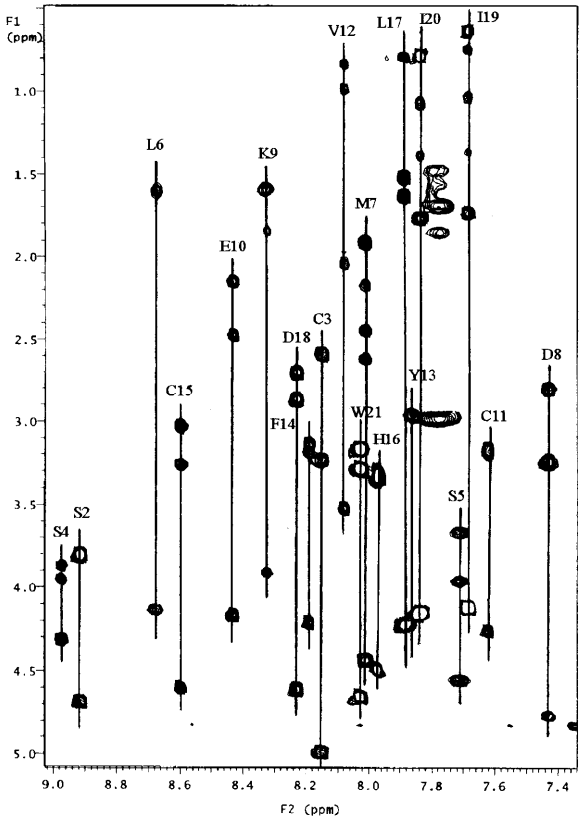

Figure 2 A section of the TOCSY spectrum (80 ms) of ET-1. The vertical lines show the individual spin-coupling connectivities with residue numbers.

The high-frequency region of the TOCSY spectrum Figure 2 clearly showed the complete side-chain proton connectivities with the NH proton but some missing side-chain connectivities for Leu^6 and Lys^9. The two serine residues, Ser^4 and Ser^5, were clearly identified on the basis of their distinctive chemical shift values of the two β-proton resonances and Ser^2 showed only a single peak for the β-protons. The two isoleucine residues, Ile^{19} and Ile^{20} showed complete side-chain connectivities through the NH proton in the COCSY spectrum. The unique Lysine, Lys^9, was identified on the basis of its distinctive αH/εH cross peak in the αH region (F_2, F_1) of the TOCSY spectrum. The complete spin pattern for the unique Val^{12} residue was observed in both the DQFCOSY and TOCSY spectra.

Two leucine residues, Leu^6 and Leu^{17}, were clearly distinguishable on the basis of their distinctive chemical shifts of their methyl resonances appearing in the αH region of the TOCSY spectrum. The TOCSY cross peaks corresponding to magnetization transfer from αH/γH through the entire spin

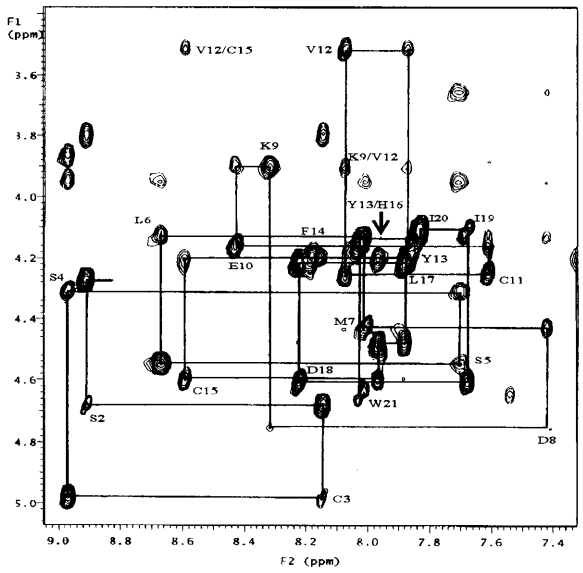

Figure 3 Fingerprint region of the NOESY spectrum (150 ms) of ET-1. Residue numbers and three long-range connectivities are indicated.

system were clearly visible for both of the unique amino acid residues Met[7] and Glu[10]. The chemical shift value for the εCH_3 of Met[7] was obtained from the one-dimensional ^{1}H-NMR spectrum. Four unique aromatic amino acid residues, Tyr[13], Phe[14], His[16] and the C-terminal end Trp[21], were clearly discriminated from the rest by aromatic-H to βH resonance connectivities in the NOESY spectrum. The individual identification and the positions of the residues were determined by direct comparison of the TOCSY and NOESY spectra.

The fingerprint region (F_2,F_1) of the NOESY spectrum (Figure 3) was used for sequence specific resonance assignments, secondary structure determination and finally for tertiary structure calculation [27]. Since Lys[9] is an unique residue, it is possible to identify Glu[10], thus resolving the Met[7] and Glu[10] ambiguity. Although the Asp[8] NH/αH cross peak did not appear in the NOESY spectrum, the sequence Leu[6]-Met[7]-Asp*8* is clear and hence Leu[17] and Asp[18] are identified by elimination. The unique C-terminal aromatic residue Tri[21] showed clear aromatic 4H/αH and 4H/βH cross peaks in the NOESY spectrum. The Asp[18]-Ile[19] sequential connectivity is clear and the sequence Leu[17]-Asp[18]-Ile[19]-Ile[20]-Trp[21] is then identified. Since Val[12] is unique, it is possible to identify its neighbours Cys[11] and Tyr[13]. There is a strong sequential connectivity between His[16] and Leu[17] identifying the His[16] and thence the neighbour Cys[15]. Although the sequential connectivity between Tyr[13] and the remaining Phe[14] could not be observed owing to degeneracy of their αH chemical shifts (Table 1, Phe[14] was easily discriminated from the other three aromatic residues which were assigned with the aid of aromatic protons to βH cross peaks in the NOESY spectrum.

The cross-peak from the terminal Cys[1]α/Ser[2]NH was clearly visible in the NOESY spectrum, thence the Cys[3] is clearly identified. A strong sequential cross peak between Cys[3] to Ser[4] thence Ser[5] completes the entire sequential connectivity of ET-1.

Almost all the side-chain spin connectivities through αH were clearly observed in the DQFCOSY and TOCSY spectra for all of the amino acid residues. A broader resonance was observed for the side chain $^+NH_3$ of Lys[9] at 7.76–7.79 ppm. Although two γH resonances were observed for Met[7], only a single γH resonance has previously been reported for methionine in a random coil peptide [27]. In contrast, two separate overlapping βH and γH resonances were observed for Glu[10]. Two degenerate βH resonances were observed for Cys[1] and Cys[11]. Although two βH resonances were observed for Ser[4] and Ser[5], only a single resonance was observed for Ser[2].

The unique amino acid residue Tyr[13] showed complete spin pattern connectivities in the TOCSY spectrum with a single overlapped βH resonance. Although the NOESY spectrum showed strong prominent spin patterns from NH resonances to the entire side chain for Leu[6] and Leu[9], the TOCSY spectrum showed only a few cross peaks (NH/βHs) for Leu[6] and Lys[9]. The high reliability of the resonance assignments was supported by the $d_{\beta N}(i,i+1)$ and $d_{NN}(i,i+1)$ connectivities for neighbouring amino acid residues (Figure 4).

In addition to the neighbouring amino acid connectivities, three long-range connectivities, $d_{\alpha N}(i,i+3)$ Lys[9]/Val[12], Val[12]/Cys[15] and Tyr[13]/His[16] and one medium-range $d_{\beta N}(i,i+2)$ Ser[5]/Mer p7 were observed in the fingerprint region of the NOESY spectrum. These $d_{\alpha N}(i,i+3)$ cross peaks indicate the possibility of forming a helix between Lys[9] and His[16]. The observation of a cross peak Lys[9]/Val[12] indicates that the helical structure in this segment of the peptide encompasses the disulphide bridge between Cys[3] and Cys[11].

High reliability of the formation of the helix was confirmed by the strong $d_{\alpha\beta}(i,i+3)$ cross peaks that appeared in the αH region (F_2,F_1) of the NOESY spectrum. Although Glu[10]/Tyr[13] and Cys[11]/Phe[14] long-range $d_{\alpha N}(i,i+3)$ cross peaks could not be distinguished owing to spectral overlap, strong

Table 1 1H Chemical Shifts[a] of ET-1 Obtained in 1:1 = CD_3OH:H_2O

Residue	NH	αH/αCH$_3$	βH/βCH$_3$	γH/γCH$_3$	δCH$_2$/δCH$_3$	εCH$_2$/εCH$_3$	Aromatics/others
1 Cys		4.29	3.29, 3.29				
2 Ser	8.91	4.69	3.81, 3.81				
3 Cys	8.15	4.99	2.59, 3.23				
4 Ser	8.97	4.32	3.87, 3.96				
5 Ser	7.71	4.55	3.66, 3.96				
6 Leu	8.68	4.14	1.62, 1.62	1.62	0.85, 0.92		
7 Met	8.01	4.44	1.91, 2.17	2.45, 2.61			
8 Asp	7.43	4.76	2.80, 3.24				
9 Lys	8.32	3.91	1.57, 1.85	1.48	1.69	2.98	$^+NH_3$, 7.76–7.79
10 Glu	8.44	4.17	2.15, 2.15	2.48, 2.48			
11 Cys	7.62	4.26	3.18, 3.18				
12 Val	8.08	3.53	2.04	0.84, 0.99			
13 Tyr	7.87	4.20	2.96, 2.96				2/6, 6.80; 3/5, 6.62
14 Phe	8.19	4.21	3.13, 3.18				2/6, 7.30; 3/5, 7.35
15 Cys	8.60	4.60	3.03, 3.27				2H, 8.57; 4H, 7.28
16 His	7.97	4.48	3.30, 3.34				2H, 8.57; 4H, 7.28
17 Leu	7.89	4.23	1.63, 1.63	1.52	0.79, 0.79		
18 Asp	8.23	4.61	2.70, 2.86				
19 Ile	7.68	4.12	1.73	0.75 1.03, 1.35	0.64		
20 Ile	7.84	4.15	1.77	0.79 1.07, 1.39	0.79		
21 Trp	8.03	4.65	3.17, 3.29				2H, 7.16; 4H, 7.55 5H, 7.03; 6H, 7.11 7H, 7.36; NH, 10.14

[a] Chemical shifts are referenced to the residual CD_2*H*OH resonance at 3.3 ppm.

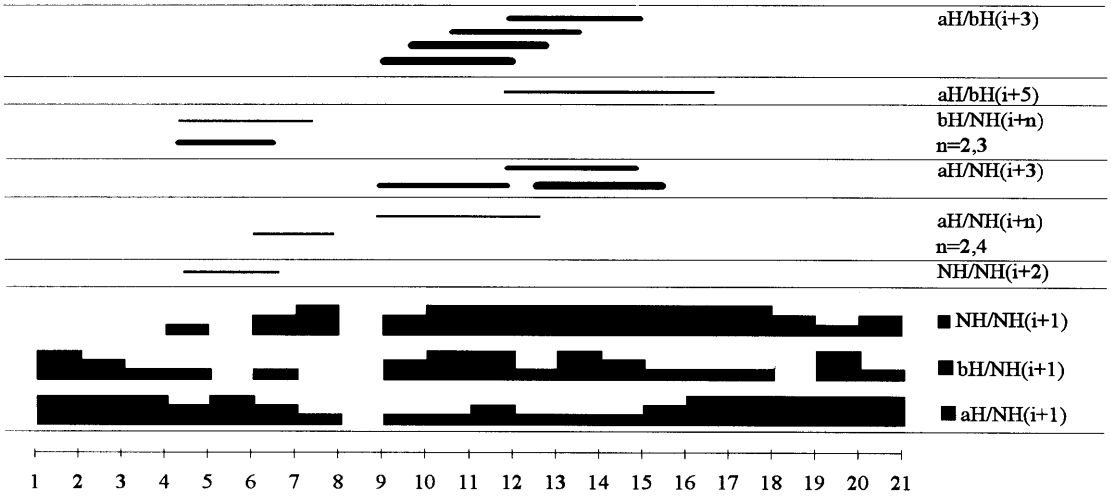

Figure 4 The amino acid sequence of ET-1 with a summary of the sequential assignments. The intensities of the NOEs are represented by the thickness of the lines and bars. aH, bH and NH are alpha, beta and amide protons respectively.

Table 2 Summary of the Solution Conformations of the Endothelin and Endothelin-like Peptides Derived from Previous NMR Studies

Peptide	Helical region	N-terminus	C-terminus	Solvent	Reference
Et-1	Undefined	Undefined	Associated with bicyclic core	d_6-DMSO	[28]
ET-1	K^9-C^{15}	Structured	Undefined	d_6-DMSO	[29]
ET-1	C^{11}-C^{15}	Undefined	Associated with bicyclic core	d_6-DMSO/TFE	[30]
[NIe^7]ET-1	K^9-H^{16}	S^5D^8	–	d_6-DMSO and 50% CD_3CN/H_2O	[31]
ET-1	L^6-C^{11}	Undefined	Undefined	d_6-DMSO	[32]
ET-1	K^9-L^{17}	S^5-D^8	Undefined	ethylene glycol/H_2O (60:40) with TFA	[33]
ET-1	K^9-C^{15}	S^5-D^8 (β-bend)	Undefined	10% d_4-AcOH/H_2O	[34]
ET-1	K^9-C^{15}	S^5-D^8	Undefined	30% CD_3-CN/H_2O	[35]
ET-1	K^9-F^{14}/C^{15}	S^5-D^8 (reverse turn)	Averaging	ethylene glycol/H_2O (60:40) with TFA	[36]
[1,15Aba]ET-1	K^9-H^{16}	S^5-D^8 (β-turn)	Structured	10% CD_3CN/H_2O with 1.5% AcOH	[37]
ET-1	K^9-C^{15}	S^5-D^8 (β-turn)	Undefined	10% d_3-AcOH/H_2O	[38]
ET-1	K^9-H^{16}	S^5-K^9 (β-turn)	Unstructured	d_6-DMSO	[39]
ET-1	K^9-H^{16}	S^5-D^8 (β-turn)	Undefined	d_3-AcOH/H_2O	[40]
[Ala^7]ET-1	K^9-H^{16}	S^5-D^8 (β-turn)	Undefined	d_3-AcOH/H_2O	[40]
[Ala^8]ET-1	K^9-H^{16}	S^5-A^8 (β-turn)	Undefined	d_3-AcOH/H_2O	[40]
ET-1	K^9-H_{16}	S^5-K^9 (β-turn)	Folds back towards the helix	H_2O	[41]
ET-3	K^9-C^{15}	–	Opposed to the bicyclic core	H_2O	[42]
ET-3	K^9-C^{15} opposite handed	β strand	Associated with bicyclic core	d_3-AcOH/H_2O	[43]
Big-ET-1	K^9-C^{15}	S^5-D^8 (β-turn)	Undefined	H_2O	[44]
Apamin	A^9-$\mathfrak{Q}^{17}$	N^2-A^5 (β-turn)	–	H_2O	[45]
Apamin	P^6-$\mathfrak{Q}^{16}$	N^2-A^5 (reverse turn)	–	H_2O	[46]
Apamin	C^3-A^5/P^6	A^9-H^{18} (reverse turn)	–	H_2O	[47]
SRTX-6b	D^8-C^{15}	C^3-M^6 (β-turn)	Undefined	CD_3-CN/H_2O	[48]
SRTX-6b	D^8-H^{16}	C^3-M^6 (β-turn)	Undefined	CD_3CN/H_2O	[49]
SRTX-6b	K^9-$\mathfrak{Q}^{17}$	Undefined	Undefined	H_2O	[50]
SRTX-6c	E^9-C^{15}	Undefined	Undefined	H_2O	[51]

$d_{\alpha\beta}(i,i+3)$ cross peaks indicated the formation of an α-helix. In addition to the above connectivities, weak $d_{\alpha N}(i,i+1)$ and strong $d_{NN}(i,i+1)$ connectivities observed in the segment of Lys^9-His^{16} also suggested the existence of an α-helix.

The H–D exchange rate of amide protons provided information concerning the hydrogen bonds in the secondary structure. Although both the terminal amide protons and some surface protons disappeared quickly in the deuterium exchange experiment, those of Met^7, Lys^9, Cys^{11}, Val^{12}, Tyr^{13}, Phe^{14} and Cys^{15} amide protons were still clearly observed after 8 min. Twenty-five minutes later, all the above amide protons were still observed except Lys^9 and Glu^{10} but all had completely disappeared after 6 h. These observations support the conclusion that a strongly hydrogen bonded segment exists in the region between Lys^9 and His^{16}.

The dependence of the chemical shifts of backbone amide protons on temperature [27] was measured over the range of 290–313 K. A structured state is indicated by the very small temperature gradient of Asp^8 $\Delta\delta/\Delta T = -0.7$ ppb/C. Smaller temperature coefficients -1.7 ppb/C for Tyr^{13} and -3.5 ppb/C for Lys^9 and His^{16} indicate shielding from solvent exchange of the amide protons of

residues 9–16 and also suggests that these protons are involved in intramolecular hydrogen bonding.

Other NOE connectivities indicating another regular structure were observed in the region between Ser^5 and Asp^8. The strong d_{NN} Met^7/Asp^8, medium $d_{\beta N}$ Ser^5/Met^7, very weak d_{NN} Asp^8/Lys^9 (seen at lower thresholds), medium $d_{\beta N}$ Ser^5/Met^7 and slow Met^7 amide proton exchange could arise from a turn structure in the Ser^5-Asp^8 region. These NOE connectivities and the $^3J_{\alpha H}$ coupling constants of Leu^6 and Met^7, the values of which are ~ 5 and 8 Hz respectively, suggest a type I β-turn conformation in this region of the peptide. The remaining parts of the ET-1 structure, especially the C-terminal region beyond His^{16}, showed a series of strong $d_{\alpha N}$ NOEs and medium $^3J_{NH\alpha}$ coupling constants (7–8 Hz) for Ile^{19}, Ile^{20} and Trp^{21}. These couplings are probably due to conformational averaging in the tail region.

Therefore four regions of structure can be defined; an internal region (residues 9–16) in which $d_{\alpha H}$ are weaker than those observed in the N- (residues 1–4) and the C- (residues 17–21) terminal regions, where the strong intensities of NOEs are in good agreement with an extended conformation and a turn region (residues 5–8). The $^3J_{\alpha H}$ coupling constants are also representative of these areas. Large values were localized at the two outer regions while smaller values (< 5.5 Hz) were observed on the internal segments.

The results obtained from CD_3OH/H_2O solution data for ET-1 are in good agreement with those published by some other research groups (Table 2. The literature reports of NH and αH chemical shifts in different solvents were compared with our results (Figure 5). Our results showed that most of the NH and αH chemical shifts lie between the documented values. All the reported NMR data for endothelins and sarafotoxins reveal that some unusual chemical shifts are always observed. In most of the cases, the Ile^{19} γCH_3 of ET-1 is shifted to low frequency suggesting a preserved structural character in all media [33–36]. This is also true for the endothelin analogue endothelin-3 (ET-3) [43] and sarafotoxin-6b in which one of Val^{19} γCH_3 signals [50] corresponds to the Ile^{19} γCH_3 group.

All calculated structures have the same backbone feature from Lys^9-His^{16} (Figure 6) in the bicyclic core region and a β-turn. Two biologically active residues Asp^8 and Val^{12}, in some cases Phe^{14}, face the bicyclic core while the residue Leu^6 always faces away from both the helical core and the bicyclic core. In addition to the common hydrogen bonds found in

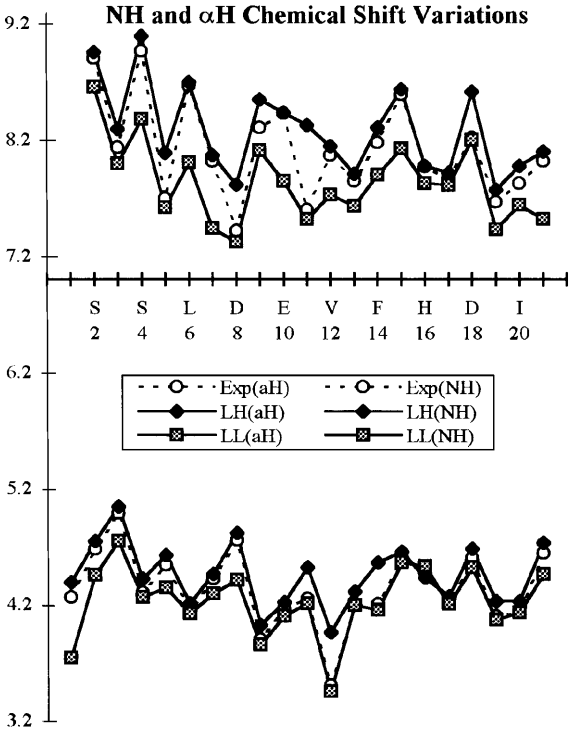

Figure 5 Comparison of the NH and αH chemical shift variations of ET-1 in different solvents Table 2 and our results: aH, αH chemical shift; NH, amide proton chemical shift; LH, literature highest chemical shift value; LL, literature lowest chemical shift value.

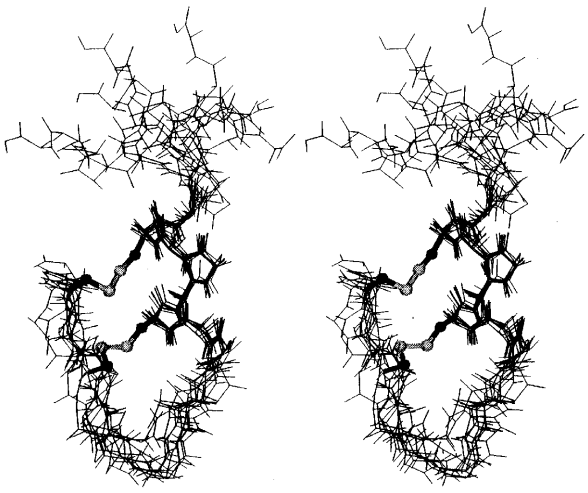

Figure 6 Stereoview of the ten averaged conformations of ET-1. Backbone atoms in the helical region (Lys^9-His^{16}) are best-fitted and the disulphide bridges only for a single conformation are shown for clarity.

the helical region, a distinct hydrogen bond was observed between Ser^5/Met^7 in most of the calculated structures.

Molecular modelling of ET-1 suggests that the disulphide constraints (1–15 and 3–11) are insufficient to restrict the formation of a helical conformation in the middle of the sequence and additinal structural features can clearly be seen in the calculated structures. It is interesting to see that the two disulphide bridges are on one side of the helix, while the other side of the helix forms a contiguous area containing important biologically active residues (13, 17 and possible 18).

The 3D structure through the Cys^1-Ser^4 segment of the polypeptide is ill-defined based on the NOE and this portion of the molecule is thought therefore to be inequilibrium among various conformational states. The conformations of the N-terminus of the calculated structures, however, are in good order from the RMSD fitting (Table 3. The side-chain groups of this region also showed the compact conformations but this is not the case for the C-terminus. Tighter disulphide bridges between 1–15 and 3–11 may support the N-terminal conformation.

Important long-range interactions between the C-terminal part of the molecule and the helix were

Table 3 Structural Statistics for the Family of Structures of ET-1

	DIANA[a]	Final[b]
Number of NOE constraints used	230	131
Number of NOE violations >0.2 Å	25	8
Number of NOE violations >0.5 Å	10	3
Constraint violations (DIANA 70.2 Å)		
Intra-residue constraints	0.409 ± 0.112	0.043 ± 0.002
Sequential constraints	0.716 ± 0.218	0.073 ± 0.004
Medium and long-range constraints	0.433 ± 0.213	0.055
0.003		
Total NOE constraints	0.519 ± 0.184	0.058
0.004		
Hydrogen bond constraints	0.340 ± 0.127	0.058 ± 0.005
Disulphide constraints	0.423 ± 0.163	0.065 ± 0.002
Torsional angle constraints $>5°$	34.60	16.30
Atomic rms differences (Å)		
Total residues (1–21)	4.69 ± 0.77	
Total backbone atoms (1–21)	3.24 ± 0.69	
Helical residues (9–16)	2.10 ± 0.29	
Helical backbone atoms (9–16)	0.60 ± 0.14	
Helical heavy atoms (9–16)	1.86 ± 0.29	
Turn residues (5–8)	1.80 ± 0.34	
Turn backbone atoms (5–8)	0.65 ± 0.18	
N-terminal residues (1–4)	1.57 ± 0.32	
C-terminal residues (17–21)	3.06 ± 0.93	
Potential energies (kcal/mol)		
Bond stretching	7.96 ± 0.45	
Angle bending	65.33 ± 3.75	
Torsional	38.74 ± 3.25	
Out-of-plane bending	0.67 ± 0.16	
1–4 van der Waals	20.96 ± 0.97	
Van der Walls	-90.87 ± 5.32	
Total	42.43 ± 8.76	

[a] DIANA is the ten solution structures obtained from the DIANA calculation. [b] Final is the mean structure obtained after the final molecular dynamics calculations.

also detected. In particular, the $Val^{12}\alpha H/Leu^{17}\beta H$, Tyr^{13}aromatics/$Leu^{17}\gamma CH_3$ and Phe^{14}aromatics/$Leu^{17}\delta CH_3$ showed intense NOESY cross peaks. In addition, the deuterium exchange experiment showed the partially bound Ile^{19} and Ile^{20} amide protons in the C-terminal tail. This would not be expected for a rapidly varying unstructured state. In contrast, $^3J_{\alpha H}$ coupling constants of the C-terminal residues indicated a random conformation. These results suggest that the C-terminal tail region has a partially structured nature. Anderson *et al* [36] have reported that the C-terminus is not the most mobile portion of the structure but motional averaging was in fact more evident in an N-terminal region Cys^1-Ser^4.

Notably dissimilar NMR structures have been proposed for ET-1 by different research groups. NMR structures of ET-1 in predominantly aqueous media show evidence of a helical region between Lys^9-$Cys^{15}/His^{16}/Leu^{17}$, but in most cases the remaining structure is ill-defined. The structure of the C-terminal region and its orientation to the bicyclic core were completely indeterminant in most reports. Despite the general similarity of all structures reported for peptides of the endothelin family, including ET-3 and sarafotoxin-6b and 6c, significant differences include the number of amino acid residues involved in the helix, the nature of the helix, the presence or absence of a turn at residues 5–8 and the conformation and degree of disorder reported for the C-terminus. It can be seen that the local RMSD values for the backbone conformation between Lys^9 and His^{16} show small variations while the N- and C-termini show considerable variations. Small global RMSD variations were also observed for helical residues. The present evidence for a helical structure (Lys^9-His^{16}) and a turn at Ser^5-Asp^8 was noted in a few cases. The structures obtained for ET-1 are in good agreement with the experimentally derived constraints. It should be noted that whatever medium is used, the ET-1 molecule seems to adopt a roughly similar structure Figure 7). All the results suggest that the endothelin assumes an ordered conformation in solution.

The crystal structure of ET-1 [53] has been described as having an N-terminal extended β-strand with a bulge between residues 5 and 7 followed by a hydrogen bonded loop between the carbonyl oxygen of residue 7 and the amide proton of residue 11. The residues 12–15 of endothelin form an irregular α-helix while C-terminal tail (residues 16–21) forms an ordered α-helical structure. In addition, the crystal structure of the tail portion is

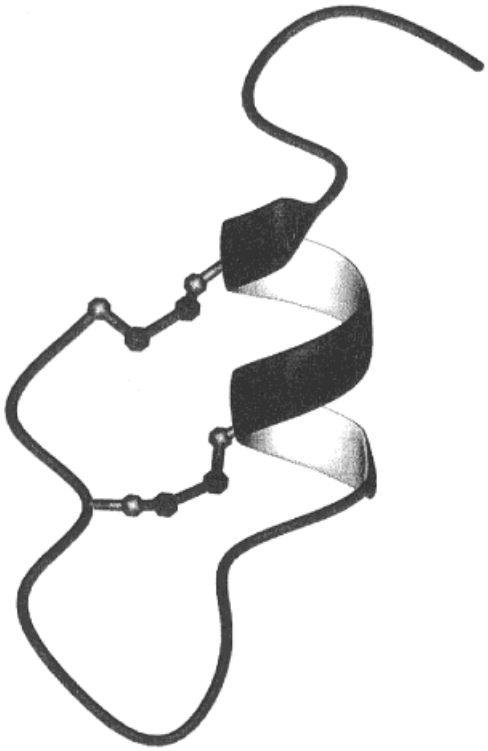

Figure 7 MOLMOL [52] cartoon drawing of ET-1 with ball and stick representation of the disulphide bridges.

neither more flexible nor more disordered than the globular head region (residues 1–15). Thus the X-ray and NMR structures do have common features but also differ significantly in detail, especially the C-terminal residues (16–21). There is little basis for assuming that either the solution structure or the crystal structure would bear a close resemblance to that observed in receptor-associated conformation(s).

A characteristic of ET-1 is the conservation of two disulphide bridges and the hydrophobic C-terminal amino acid residues, which are considered to be important for the expression of its biological activities [54]. Kimura *et al* [9] reported that the vasoconstrictor activity of endothelin is considerably decreased by the removal of the C-terminal Trp^{21} residue. A systematic study of ET-1{X21} has revealed that only phenylalanine and tyrosine resulted in ten-fold loss in activity indicating the importance of the aromatic group at the end of the peptide [54]. In the models obtained from this study, a biologically active Trp^{21} residue which is located at the end of the C-terminal tail is isolated and

separated from all the other residues. It is unlikely that the removal of Trp^{21} causes a considerable conformational change over the molecule leding to loss in activity. Therefore Trp^{21} itself would be recognized by the receptor(s).

ET has multiple binding sites on various kinds of cell membranes including smooth muscle, epithelial and endothelial cells. Two ET receptor subtypes, termed ET_A and ET_B were first identified and, recently, an ET-3 specific receptor, ET_C, was cloned and characterized. It is not known whether the ET_C receptor is present in mammalian species. It is well known [56] that the two disulphide bridges are required for receptor binding and vasoconstrictor activity. Synthetic truncated analogues of ET such as porcine ET1-15 or ET16-21 do not show vasoconstrictor activities [57] nor receptor binding activities [58]. These observations suggest that the receptor(s) for ET-1 recognize(s) an active conformation consisting of both the helical core (9–16) and the tail (18–21) region. The results obtained from this study did not show the interaction between the core and the tail portions in solution. It seems likely that the receptor bound conformation of ET-1 is different from that in solution.

CONCLUSIONS

Some less polar solvents (methanol, dimethylsulphoxide) or solvent mixtures such as water/methanol and water/trifluroethanol tend to induce more structure formation in peptides. These solvents offer additional advantages (good solubility, less aggregation) and cases where a mixed solvent is used, the lower concentration of water eases the problems associated with NMR experiments. Whatever the conditions used for structure determination of endothelin and endothelin-like peptides, most of the calculated structures show general similarities; a turn structure in the N-terminus, a helical structure in the middle and undefined tail at the end. However, bioassay results indicate that, in most cases, the C-terminal region plays an important part in receptor binding and functional activity. Structure calculations suggest that the ET-1 molecule assumes an ordered structure in solution.

Acknowledgements

We are grateful to the Commonwealth Association and the British Council for generous funding to C.M.H. The Engineering and Physical Science Research Council (EPSRC) for 600 MHz NMR facilities and the Wellcome Trust for molecular modelling facilities at the University of Edinburgh are also acknowledged. We wish to thank Kevin Shaw and Brian Whigham for technical assistance with the synthesis of ET-1. Thanks are also due to Parke Davis Pharmaceuticals for financial support and providing a sample of natural ET-1 for comparison with the synthetic material.

REFERENCES

1. M. Yanagisawa, H. Kurihara, S. Kimura, Y. Tomobe, M. Kobayashi, Y. Mitsui, Y. Yazaki, K. Goto and T. Masaki (1988). A novel potent vasoconstrictor peptide produced by vascular endothelial cells. *Nature 332* , 411–415.
2. T. Masaki, M. Yanagisawa, A. Inoue, Y. Takuwa, K. Goto and S. Kimura (1990). Biological activity of endothelin. *J. Cell. Biol. Chem. 14* E, 199.
3. M. Yanagisawa and T. Masaki (1989). Molecular biology and biochemistry of the endothelins. *Trends Pharmacol. Sci. 10*, 374–378.
4. Y. Itoh, M. Yanagisawa, S. Ohkubo, S. Kimura, T. Kosaka, A. Inoue, N. Ishida, Y. Mitsui, H. Onda and M. Fujino (1988). Cloning and sequence analysis of cDNA encoding the precursor of a human endothelium-derived vasoconstrictor peptide, endothelin: identity of human and procine endothelin. *FEBS Lett. 231*, 440–444.
5. X.-M. Cheng, S. S. Nikam and A. M. Doherty (1994). Development of agents to modulate the effects of endothelin. *Curr. Med. Chem. 1*, 271–312.
6. G. M. Rubanyi and M. A. Polokoff (1994). Endothelins: Molecular biology, biochemistry, pharmacology, physiology, and pathophysiology. *Pharm. Rev. 46*, 325–415.
7. P. W. Erhardt in: *Endothelin Structures and Structure Activity Relationships* G. M. Rubanyi, Ed., p. 41–57, Oxford University Press, New York 1992.
8. D. M. Leonard, M. D. Reily, J. B. Dunbar, K. E. Holub and W. L. Cody (1995) Structure–activity and biophysical studies of the C-terminal hexapeptide of endothelin. *Bioorg. Med. Chem. Lett. 5*, 967–972.
9. S. Kimura, Y. Kasuya, T. Sawamura, O. Shinmi, Y. Sugita, M. Yanagisawa, K. Goto and T. Masaki (1988). Structure activity relationship of endothelin: Importance of the C-terminal moiety. *Biochem. Biophys. Res. Commun. 156*, 1182–1186.
10. R. Bazzo, M. J. Tappin, A. Pastore, T. S. Harvey, J. A. Carver and I. D. Campbell (1988). The structure of melittin. A. ^{1}H-NMR study in methanol. *Eur. J. Biochem. 173*, 139–146.
11. L. Jiang, 'The chemical synthesis of peptides with biological importance', PhD Thesis, University of Edinburgh 1996.

12. A. J. Shaka and R. Freeman (1983). Simplification of NMR spectra by filtration through multiple-quantum coherence. *J. Magn. Reson. 51*, 169–173.
13. A. Bax and D. G. Davis (1985). MLEV-17 based two-dimensional homonuclear magnetisation transfer spectroscopy. *J. Magn. Reson. 65*, 355–360.
14. A. Kumar, R. R. Ernst and K. Wüthrich (1980). A two-dimensional nuclear Overhauser enhancement experiment for the elucidation of complete proton–proton cross-relaxation networks in biological macromolecules. *Biochem Biophys. Res. Commun. 95*, 1–6.
15. D. J. States, R. A. Haberkorn and D. J. Ruben (1982). A two-dimensional nuclear Overhauser experiment with pure absorption phase in four quadrants. *J. Magn. Reson. 48*, 286–292.
16. Tripos Molecular Modelling Software, SYBYL ver. 6.1, Tripos Associates, St Louis, MO, USA.
17. M. Billeter, W. Braun and K. Wüthrich (1982). Sequential resonance assignments in protein ^{1}H nuclear magnetic resonance spectra. *J. Mol. Biol. 155*, 321–346.
18. K. Wüthrich, M. Billeter and W. Braun (1983). Pseudo-structures for the 20 common amino acids for use in studies of protein conformations by measurements of intramolecular proton–proton distance constraints with nuclear magnetic resonance. *J. Mol. Biol. 169*, 949–961.
19. M. P. Williamson, T. F. Havel and K. Wüthrich (1985). Solution conformation of proteinase inhibitor IIA from bull seminal plasma by ^{1}H nuclear magnetic resonance and distance geometry. *J. Mol. Biol. 182*, 295–315.
20. P. Güntert, W. Braun and K. Wüthrich (1991). Efficient computation of three-dimensional protein structures in solution from nuclear magnetic resonance data using the program DIANA and the supporting programs CALIBA, HABAS and GLOMSA. *J. Mol. Biol. 217*, 517–530.
21. M. Clark, R. D. Cramer III and N. van Opdenbosch (1989). Validation of the general purpose Tripos 5.2 force field. *J. Comp. Chem. 10*, 982–1012.
22. S. Kumagaye, H. Kuroda, K. Nakajima, T. X. Watanabe, T. Kimura, T. Masaki and S. Sakakibara (1988). Synthesis and disulphide structure determination of procine endotheline: an endothelium derived vasoconstricting peptide. *Int. J. Peptide Protein Res. 32*, 519–526.
23. F. C. A. Gaeta, L. B. Slater, B. R. Sunday, J. R. Miller, C. L. Ramsaur, L. Ghibaudi and M. Chatterjee in: *Proceedings of the Eleventh American Peptide Symposium* J. E. Rivier and G. R. Marshall, Eds., p. 264–266, ESCOM, Leiden 1990.
24. K. Akaji, H. Nishiuchi and Y. Kiso (1995). Synthesis of human endothelin-1 by regioselective disulphide formation using silyl chloride-sulphoxide system. *Tetrahedron Lett. 36*, 1875–1878.
25. W. Liu, G. H. Shiue and J. P. Tam in: *Proceedings of the Eleventh American Peptide Symposium* J. E. Rivier and G. R. Marshall, Eds., p. 271–273, ESCOM, Leiden 1990.
26. R. Ramage, G. W. Biggin, A. R. Brown, A. Comer, A. Davidson, L. Draffan, L. Jiang, G. Morton, N. Robertson, K. T. Shaw, G. Tennant, K. urquhart and J. Wilkin in: *Proceedings of the Fourth International Symposium: Innivation and perspectives in solid phase synthesis and combinatorial chemical libraries*, R. Epton, Ed., p. 1–10, Mayflower, Birmingham 1996.
27. K. Wüthrich: in: *NMR of Proteins and Nucleic Acids*, Wiley, New York 1986.
28. V. Saudek, J. Hoflack and J. T. Pelton (1989). *1*H-NMR study of endothelin, sequence-specific assignment of the spectrum and a solution structure. *FEBS Lett. 257*, 145–148.
29. S. Endo, H. Innoka, Y. Ishibashi, C. Kitada, O. Mizuta and M. Jufino (1980). Solution conformation of endothelin determined by nuclear magnetic resonance and distance geometry. *FEBS Lett. 257*, 149–154.
30. V. Saudek, J. Hoflack and J. T. Pelton (1991). Solution conformation of endothelin-1 by ^{1}H NMR, CD and molecular modelling. *Int. J. Peptide Protein Res. 37*, 174–179.
31. A. Aumelas, L. Chiche, E. Mahe, D. L-Nguyen, P. Sizun, P. Berthault and B. Perly (1991). Determination of the structure of [Nle7]-endothelin by ^{1}H NMR. *Int. J. Peptide Protein Res. 37*, 315–324.
32. S. L. Munro, D. J. Craik, D. McConville, J. G. hall, M. Searle, W. Bicknell, D. Scanlon and C. Chandler (1991). Solution conformation of endothelin, a potent vaso-constricting bicyclic peptide. *FEBS Lett. 278*, 9–13.
33. S. R. Krystek, D. A. Bassolino, J. Novotny, C. Chen, T. M. Marschner and N. H. Andersen (1991). Conformation of endothelin in aqueous ethylene glycol determined by ^{1}H-NMR and molecular dynamics simulations. *FEBS Lett. 281*, 212–218.
34. H. Tamoaki, Y. Kobayashi, S. Nishimura, T. Ohkubo, Y. Kyoguku, K. Nakajima, S. Kumagaye, T. Kimura and S. Sakakibara (1991). Solution conformation of endothelin determined by means of *1*H-NMR spectroscopy and distance geometry calculations. *Protein Eng. 4*, 509–518.
35. M. D. Reily and J. B. Dunbar (1991). The conformation of endothelin-1 in aqueous solution: NMR-derived constraints combined with distance geometry and molecular dynamics calculations. *Biochem. Biophys. Res. Commun. 178*, 570–577.
36. N. H. Andersen, C. Chen, T. M. Marschner, S. R. Krystek and D. A. Bassolino (1992). Conformational isomerism of endothelin in acidic aqueous media: A quantitative NOESY analysis. *Biochemistry 31*, 1280–1295.
37. M. Coles, S. L. A. Munro and D. J. Craik 91994). The solution structure of a monocyclic analogue ofendothelin [1,15 Aba]-ET-1, determined by ^{1}H NMR spectroscopy. *J. Med. Chem. 37*, 656–664.

38. Y. Kobayashi in: *Proceedings of the Eleventh American Peptide Symposium*, J. E. Rivier and G. R. Marshall, Eds., p. 552–556, ESCOM, Leiden 1990.
39. S. C. Brown, M. L. Donlan and P. W. Jeffs in: *Proceedings of the Eleventh American Peptide Symposium*, J. E. Rivier and G. R. Marshall, Eds., p. 595–597, ESCOM, Leiden 1990.
40. D. C. Dalgarno, L. Slater, S. Chackalamannil and M. M. Senior (1992). Solution conformation of endothelin and point mutants by nuclear magnetic resonance spectroscopy. *Int. J. Peptide Protein Res. 40*, 515–523.
41. E. Ragg, R. Mondelli, S. Penco, G. Bolis, L. baumer, and G. Guaragna (1994). Tertiary structure of endothelin-1 in water by ^{1}H NMR and molecular dynamics studies. *J. Chem. Soc. Perkin Trans. 2*, 1317–1326.
42. R. G. Mills, S. L. O'Donoghue, R. Smith and G. F. King (1992). Solution structure of endothelin-3 determined using NMR spectroscopy. *Biochemistry 31*, 5640–5645.
43. P. Bortmann, J. Hoflack, J. T. Pelton and V. Saudek (1991). Solution conformation of endothelin-3 by ^{1}H NMR and distance geometry calculations. *Neurochem. Int. 18*, 491–496.
44. M. L. Donlan, F. K. Brown and P. W. Jeffs (1992). Solution conformation of human big endothelin-1. *J. Biomol. NMR 2*, 407–420.
45. J. H. Pease and D. E. Wemmer (1988). Solution structure of apamin determined by nuclear magnetic resonance and distance geometry. *Biochemistry 27*, 8491–8498.
46. V. F. Bystrov, V. V. Okhanov, A. I. Miroshnikov and Y. A. Ovchinnikov (1980). Solution spatial structure of apamin as derived from NMR study. *FEBS Lett. 119*, 113–117.
47. D. Wemmer and N. R. Kallenback (1983). Structure of apamin in solution: A two-dimensinal nuclear magnetic resonance study. *Biochemistry 22*, 1901–1906.
48. A. Aumelas, L. Chiche, E. Mahe, D. Le-Nguyen, P. Sizun, P. Berthault and B. Perly (1991). ^{1}H NMR study of the solution structure of sarafotoxin-S6b. *Neurochem. Int. 18*, 471–475.
49. A. F. Atkins, R. C. Martin and R. Smith (1995). *1*H NMR studies of sarafotoxin SRTb, a nonselective endothelin receptor agonist, and IRL 1620, an ET_B receptor-specific agonist. *Biochemistry 34*, 2026–2033.
50. R. G. Mills, A. R. Atkins, T. Harvey, F. K. Junius, R. Smith and G. F. King (1991). Conformation of sarafotoxin-6b in aqueous solution determined by NMR spectroscopy and distance geometry. *FEBS Lett. 282*, 247–252.
51. R. G. Mills, G. B. Ralston and G. F. King (1994). The solution structure of sarafotoxin-c. *J. Biol. Chem. 269*, 23413–23419.
52. R. Karadi, M. Billeter and K. Wüthrich (1996). A program for display and analysis of macromolecular structures. *J. Mol. Graphics. 14*, 51–55.
53. R. W. Janes, D. H. Pepaus and B. A. Wallace (1994). The crystal structure of human endothelin. *nature Struct. Biol. 1*, 311–319.
54. 54.K. Nakajima, S. Kubo, S. Kumagaye, H. Nishio, M. Tsunmi, T. Inui, H. Kuroda, N. Chino, T. X. Watanabe, T. Kimura and S. Sakakibara 91989). Structure activity relationships of endothelin. *Biochem. Biophys. Res. Commun. 163*, 424–429.
55. T. Koshi, C. Suzuki, K. Arai, T. Mizoguchi, T. Torii, M. Hirata, M. Ohkuchi and T. Okabe (1991). Syntheses and biological activities of endothelin-1 analogues. *Chem. Pharm. Bull. 39*, 3061–3063.
56. K. Kitazumi, T. Shiba, K. Nishiki, Y. Furukawa, C. Takasaki and K. Tasaka (1990). Structure–activity relationship in vasoconstrictor effects of sarafotoxins and endothelin-1. *FEBS Lett. 260*, 269–272.
57. S.-I. Kumagaye, K. Nakajima, H. Nishio, H. Kuroda, T. X. Watanabe, T. Kimura, T. Masaki and S. Sakakibara in: *Peptide Chemistry*. p. 215–220, Protein Research Foundation, Osaka, Japan 1988.
58. Y. Hirata, H. Yoshimi, T. Emori, M. Shichiri, F. Marumo, T. X. Watanabe, S.-I. Kumagaye, K. Nakajima, T. Kimura and S. Sakakibara (1989). Receptor binding activity and cytosolic free calcium response by synthetic endothelin analogues in cultured rat vascular smooth muscle cells. *Biochem. Biophys. Res. Commun. 160*, 228–234.

